

HOW TO MERGE MULTIMODAL MODELS OVER TIME?

Anonymous authors

Paper under double-blind review

ABSTRACT

Model merging combines multiple “expert” models finetuned from a base foundation model on diverse tasks and domains into a single, more capable model. However, most existing model merging approaches assume that all experts are available simultaneously. In reality, new tasks and domains emerge over time, requiring strategies to integrate the knowledge of expert models as they become available: a process we call *temporal model merging*. The temporal dimension introduces unique challenges not addressed in prior work, raising new questions such as: when training for a new task, should the expert model start from the merged past experts or from the original base model? Should we merge all models at each time step? Which merging techniques are best suited for temporal merging? Should different strategies be used to initialize the training and deploy the model? To answer these questions, we propose a unified framework called TIME (Temporal Integration of Model Expertise) which defines temporal model merging across three axes: (1) initialization, (2) deployment, and (3) merging technique. Using TIME, we study temporal model merging across model sizes, compute budgets, and learning horizons on the FoMo-in-Flux benchmark. Our comprehensive suite of experiments across TIME allows us to build a better understanding of current challenges and best practices for effective temporal model merging.

1 INTRODUCTION

Foundation models consolidate a wide range of capabilities and knowledge into a single, large model. Consequently, model merging (Regent’s et al., 1996; Wortsman et al., 2022a) has emerged as a key technique for unifying multiple task-specific specialist models derived from a shared base into a single, generalist model.

Current model merging approaches typically assume a fixed base model that is fine-tuned independently on k diverse tasks and domains to produce a set of *independent* experts (Garipov et al., 2018; Rofin et al., 2022; Ilharco et al., 2022; Yadav et al., 2023; Li et al., 2022), which are then merged simultaneously. Research in this field has therefore focused on improving merging techniques for larger or structurally different k -sets, exploring the impact of the diversity and scale of finetuning domains, tasks and experts.

However, the world is constantly evolving, leading to continuous shifts over data distributions, domains, and tasks, with new concepts emerging that may have been insufficiently covered during large-scale pretraining (Koh et al., 2021; Hu et al., 2022; Pratt et al., 2023; Menon & Vondrick, 2023; Zhang et al., 2021; Gui et al., 2024). This dynamic nature of real-world applications motivates a hitherto missing systematic exploration into *temporal model merging* (see Fig. 1) to better understand model merging along an additional, understudied axis: *time* (Zhou et al., 2024; Don-Yehiya et al., 2022). Specifically, in this work, we ask: (1) What is the best merging strategy to initialize each expert model before training? (2) What is the best merging strategy to deploy each expert model after training? (3) Which model merging techniques are most suitable for temporal merging? To answer these questions, we propose a unified framework for studying temporal model merging:

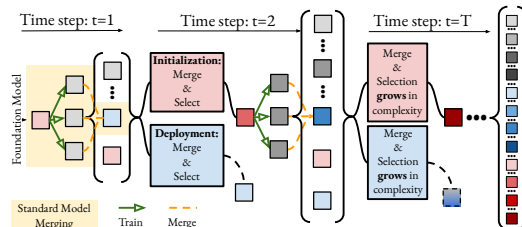


Figure 1: **Temporal Model Merging** generalizes standard model merging (yellow), which merges multiple trained experts once, in a single step. Our study reveals that initialization and deployment strategies are crucial in the temporal setting.

054
055
056
057
058
059
060
061
062
063
064
065
066
067
068
069
070
071
072
073
074
075
076
077
078
079
080
081
082
083
084
085
086
087
088
089
090
091
092
093
094
095
096
097
098
099
100
101
102
103
104
105
106
107

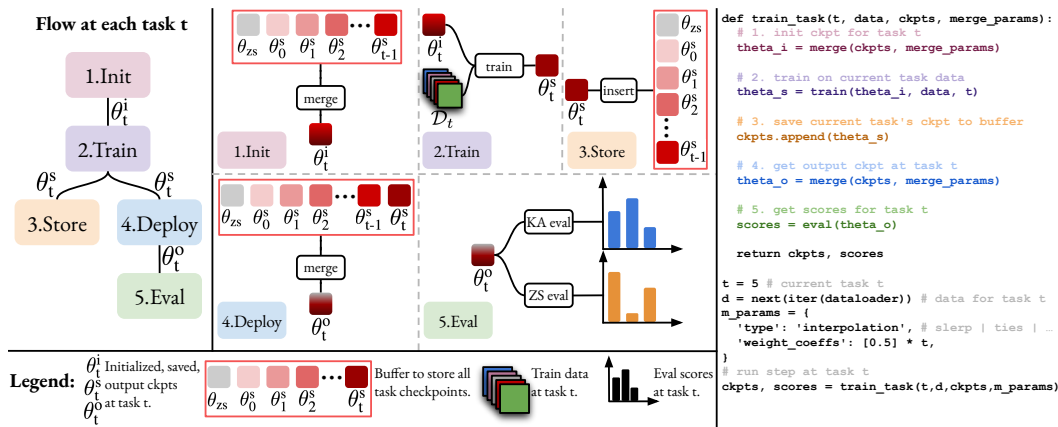


Figure 2: **Design Space of Temporal Model Merging through TIME.** We showcase our framework for the per-task pipeline of temporal model merging over multiple tasks: At each task t , we first initialize the current checkpoint to start training from, θ_t^i , by using one or more previously stored checkpoints from previous tasks, either directly or by merging them. We train θ_t^i on current task data \mathcal{D}_t to yield the current task checkpoint θ_t^s , which is inserted into the checkpoint buffer. Finally, to produce the output model, θ_t^o , we either merge previously stored checkpoints from the buffer or use them directly. The entire framework is depicted in the pseudo-code on the right panel.

TIME (Temporal Integration of Model Expertise). It is structured around three key axes spanning the design space of temporal merging solutions (as shown in Fig. 2): the choice of past checkpoints to merge before training on the current task (initialization), the choice of past checkpoints to merge after training on the current task (deployment), and the choice of the merging technique. Using our TIME framework, we position existing model merging approaches along each key axis and conduct a systematic study of model merging over time. For this, we leverage the multimodal FoMo-in-Flux by Roth et al. (2024b), a benchmark comprising 63 datasets with well-documented sequential properties, enabling a thorough investigation of temporal model merging under practical compute constraints. Our experiments systematically explore different merging techniques, initialization, and deployment strategies, providing several key insights:

Key Insights for Temporal Model Merging

- [A] Accounting for time is crucial.** Standard “offline” model merging techniques do not generalize well to the temporal merging setting (Sec. 3.1).
- [B] Complex merging techniques matter little.** Choosing sophisticated merging techniques beyond simple weighted averaging provides at best marginal benefits for temporal model merging, especially for long task sequences (Sec. 3.3).
- [C] Initialization and deployment are critical.** Choosing how to select and combine available weights before and after each task t is most important for temporal model merging (Sec. 3.2).
- [D] Temporal model merging scales well.** Larger models or compute budgets allows greater benefits from temporal merging. Scaling enables temporal model merging to even outperform the multitask model, trained on all tasks at once (Sec. 3.4).

2 DESIGN SPACE OF TEMPORAL MODEL MERGING

Notation. Throughout this work, we use t to refer to a given task at time t . Full model parameterization is denoted by θ , with the following key instantiations: θ_t represents model weights at task t , while θ_t^i , θ_t^s , and θ_t^o denote weights used for *initialization*, *saved* weight checkpoints at task t (i.e. the trained expert models), and the *output* deployed model weights, respectively. Note that while standard model merging considers model weights as elements of a fixed set $\{\theta_k\}_{k=1}^K$, temporal model merging organizes them along the time axis θ_t .

Table 1: Comparison of model merging techniques.

Method	Sparsification	Consensus	Scaling
Weight averaging Regent’s et al. (1996); Wortsman et al. (2022a)	✗	Linear Int.	Weight coeff.
SLERP Ramé et al. (2024)	✗	Spherical Int.	Weight coeff.
Task Arithmetic Ilharco et al. (2023)	✗	Linear Int.	Scaling factor
MagMax Marczak et al. (2024)	✗	Max. Magnitude	Scaling factor
TIES Yadav et al. (2023)	Top-k	Sign Agreement	Scaling factor
DARE-TIES Yu et al. (2024)	Random	Sign Agreement	Scaling factor
Breadcrumbs-TIES Davari & Belilovsky (2025)	Top/Bottom-k	Sign Agreement	Scaling factor
Model Stock Jang et al. (2024)	✗	Geometric	Adaptive ratio
LiNeS Wang et al. (2024a)	✗	✗	Layer weights

2.1 TEMPORAL MODEL MERGING THROUGH TIME

Standard model merging is typically performed offline, after all experts have been trained to convergence. In contrast, model merging in continual pretraining is generally done sequentially, using past checkpoints. Both approaches are specific instances of our more general temporal merging framework, TIME, which defines temporal merging along *three key axes*: initialization of each expert, merging for deployment at step t , and merging techniques f_{merge} applied over time:

AXIS 1: INITIALIZATION

As expert models are created continuously over time, initialization becomes a crucial choice. Unlike model merging at a single point in time, the number of potential starting points grows exponentially over time as new experts are created. This raises the question: should starting points for each time step be derived from the base weights (as in traditional merging), from a merged combination of previous experts, or from most recent weights? In this work, we study the following initialization protocols at time step t for TIME: **(1)** `initZS`, which consistently initializes with the base zero-shot model weights θ_0 at each timestep t ; **(2)** `initFT`, which at step t always initializes with the latest available finetuned model weights θ_{t-1}^S ; and **(3)** `initEMA`, which computes an unrolled exponential moving average merge over all previously seen expert models $\{\theta_{t'}^S\}_{1, \dots, t-1}$ following the equation:

$$\theta_{t'}^{\text{EMA}} = f_{\text{merge}}(\theta_{t'-1}^{\text{EMA}}, \theta_{t'-1}^S, \mathcal{F}) \quad (1)$$

with merging hyperparameters \mathcal{F} . Consequently, the initialization weights are given as $\theta_t^I = \theta_t^{\text{EMA}}$.

AXIS 2: DEPLOYMENT

With each update iteration and expert training phase t , a decision must be made on the final model to deploy, determining which weights to present for downstream use. In continual pretraining, the trained model θ_t^S is deployed directly. In contrast, standard model merging applies a merging technique f_{merge} to a fixed set of k expert models. Temporal model merging, however, must account for both previously deployed models and the growing number of expert models available over time. Unlike standard merging, where k remains constant, the number of experts to merge increases with each step. As a result, temporal merging introduces the idea of weighted combinations, balancing recent updates with retained past knowledge to achieve adaptability and stability—both critical for effective continual learning (Kirkpatrick et al., 2017; Zenke et al., 2017). In this work, we study three strategies for model deployment: **(1)** `deployFT`, which always deploys the latest finetuned expert model at step t , i.e., $\theta_t^O = \theta_t^S$; **(2)** `deployEMA`, which computes an unrolled exponential moving average merge over all expert models, i.e., $\theta_t^O = \theta_{t+1}^{\text{EMA}}$ following Eq. (1); and **(3)** `deployALL`, which applies a merging technique f_{merge} over all previously computed expert models $\{\theta_{t'}^S\}_1^{t-1}$.

AXIS 3: MERGING TECHNIQUES

At each point in time, for both initialization and deployment, merging technique f_{merge} defines *how* to combine the available expert models and checkpoints. In this work, we study nine different variants in total, shown in Tab. 1. Please refer to Appendix B for details.

2.2 COMPLETE TEMPORAL MODEL MERGING PIPELINE

Incorporating all three axes of temporal model merging, we define a five-stage update pipeline for each task t (see Fig. 2), consisting of the following steps: **(1) Init:** choose one of the aforementioned initialization protocols— init_{ZS} , init_{FT} , or init_{EMA} . This produces initialization weights θ_t^I at task t ; **(2) Train:** given θ_t^I , train on current task data \mathcal{D}_t within a set compute budget to produce the expert model θ_t^S ; **(3) Store:** append θ_t^S to storage of expert model weights \mathcal{S} ; **(4) Deploy:** choose a deployment protocol: $\text{deploy}_{\text{FT}}$, $\text{deploy}_{\text{EMA}}$, or $\text{deploy}_{\text{ALL}}$, and produce the output weights $\theta_t^O = \text{deploy}(\mathcal{S})$; and **(5) Eval:** the deployed θ_t^O is used for downstream applications and, in our case, extensive evaluation. Note that particular choices of init , deploy and f_{merge} correspond to existing approaches, for example $(\text{init}_{\text{ZS}}, \text{deploy}_{\text{ALL}}, f_{\text{merge}}^{\text{WA}})$ simply recovers offline merging through weight averaging over experts models derived from original base weights θ_0 for each task t . Similarly, $(\text{init}_{\text{FT}}, \text{deploy}_{\text{EMA}}, f_{\text{merge}}^{\text{WA}})$ recovers exponential moving average approaches as done in Stojanovski et al. (2022); Roth et al. (2024b).

3 EXPERIMENTS

Training at task t . We continuously finetune and merge a ViT-B/16 CLIP Radford et al. (2021); Cherti et al. (2022) model using the standard CLIP objective. The model is pretrained on LAION-2B (Schuhmann et al., 2022). We fix the training steps for each task based on the DataComp-Small budget of 1.8×10^9 GFLOPS, split equally across 20 tasks. At each step, we allow unrestricted access to a pretraining data pool \mathcal{P} , using the same 2M random subset of LAION-400M as in Roth et al. (2024b). We use a cosine-decay LR schedule with a linear warmup of 10%, AdamW optimizer Loshchilov & Hutter (2017), a batch size of 512 and gradient norm clipping to 1. All experiments use PyTorch Paszke et al. (2019), and are run on a compute cluster using NVIDIA A100/H100s.

Evaluation and Metrics. We use the continual pretraining benchmark Fomo-in-Flux by Roth et al. (2024b). It includes 41 adaptation datasets and 22 separate evaluation datasets, covering visual and semantic distribution shifts. We focus on two aspects: the level of *adaptation*, reflecting performance improvement with each merging step, and *retention*, capturing the preservation of prior knowledge. Specifically, we report two metrics following Roth et al. (2024b): Knowledge Accumulation (\mathcal{A}_{KA}), the average accuracy (or recall@5 for retrieval) across all 41 adaptation datasets, and Zero-Shot Retention (\mathcal{A}_{ZS}), the zero-shot accuracy or recall@5 on all 22 held-out evaluation datasets. Additional details can be found in the supplementary.

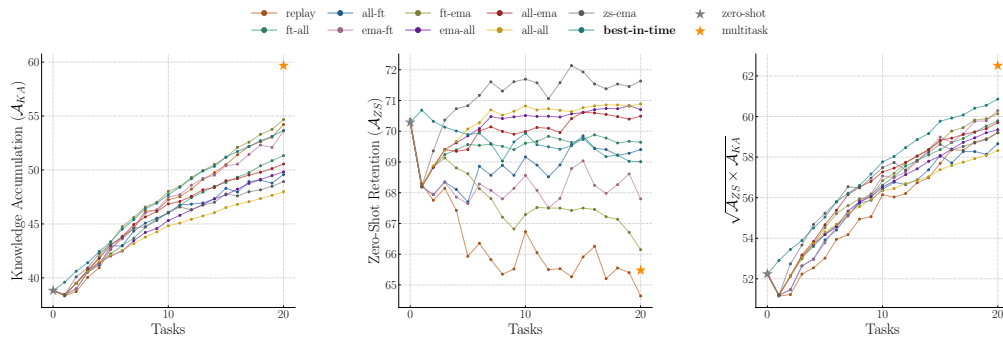
3.1 DO WE NEED MODEL MERGING ACROSS TIME?

The simplest approach to temporal merging is to disregard the time axis and follow the standard *offline* merging paradigm. In TIME terms, this corresponds to a configuration of $(\text{init}_{\text{ZS}}, \text{deploy}_{\text{ALL}}, f_{\text{merge}})$, which always fine-tunes the initial base weights θ_0 . To study the effectiveness of this strategy, we test it with various choices of f_{merge} in Fig. 6, including *averaging*, *task-arithmetic*, *magmax*, *ties*, *dare-ties*, *breadcrumbs-ties*, and *lines-ties*. For context, we include **(1)** a simple continual fine-tuning baseline (*replay*), which replays on both pretraining and previous task data, **(2)** initial zero-shot (θ_0) performance lower bound, and **(3)** multitask training upper bound. We visualize trajectories over time for knowledge accumulation \mathcal{A}_{KA} , zero-shot retention \mathcal{A}_{ZS} , and the geometric mean. Our results show that there are marginal differences between merging techniques when deployed in an offline manner for a temporal problem, and they all trace similar trajectories in the \mathcal{A}_{KA} and \mathcal{A}_{ZS} space and achieve similar final performance. Overall, however, unlike straightforward continual fine-tuning (*replay*), offline merging with *any* technique fails to address the temporal aspects of the problem, particularly struggling to consistently acquire new knowledge over time (as shown in Fig. 6, left).

3.2 TIME TRAVEL

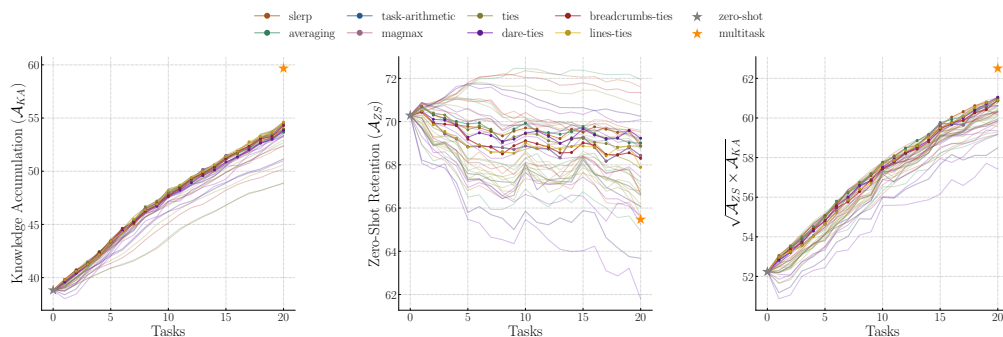
Since offline merging is ill suited to the temporal setting, we systematically explore the design space for temporal merging methods by testing all valid combinations of three initialization protocols and three deployment protocols described in Sec. 2.2. After discarding incompatible pairs, such as

216
217
218
219
220
221
222
223
224
225
226



227 **Figure 3: A journey through TIME.** We explore various initialization and deployment protocols, finding that the EMA initialization-deployment strikes the best balance between knowledge accumulation and zero-shot retention. We refer to this strategy as *Best-in-TIME*.

230
231
232
233
234
235
236
237
238
239
240



241 **Figure 4: Sweeping *Best-in-TIME*.** All merging techniques perform well with the *Best-in-TIME* strategy. Indeed, there are no significant differences between techniques, indicating that initialization and deployment matter more for temporal merging.

244 init_{ZS} with deploy_{FT} , we evaluated the remaining eight variants using weight averaging as the merging technique. As shown in Fig. 3, the choice of initialization and deployment strategy largely determines performance, significantly affecting both knowledge accumulation and retention. One combination that stands out consistently is init_{EMA} with deploy_{EMA} . This supports the findings of Stojanovski et al. (2022); Roth et al. (2024b) on small-scale continual learning and pretraining.

249 As the application of EMA model merging achieves a notably better balance between knowledge accumulation and retention than other methods, we call this approach *Best-in-TIME*. In the next section, we will explore the robustness of this strategy across different merging techniques. Please refer to Appendix E for additional EMA experiments.

254 3.3 WHAT IS THE BEST MERGE FOR BEST-IN-TIME?

256 Having identified the optimal initialization and deployment merging strategy, we now investigate the robustness of our finding by sweeping over merging techniques. In particular, we test 7 different merging techniques while keeping the *Best-in-TIME* initialization and deployment strategy. From Fig. 4, it is clear that all merging techniques perform very similarly. This indicates that, over a sufficiently long time horizon, all techniques converge to a similar behavior, echoing our results in Sec. 3.1. However, we do notice higher variance in the retention metric (\mathcal{A}_{ZS}).

263 3.4 SCALING UP TEMPORAL MODEL MERGING

264 We next scale temporal model merging up across three-axes: *model size*, *compute budget*, and *number of tasks* (results in Fig. 5 and Appendix E.2). All our experiments use the *Best-in-TIME* setup described previously, conducting hyperparameter-optimal EMA at each task.

268 **Scaling the Model.** As we increase the model scale from $S/16$ (62.3M parameters) to $B/16$ (149.6M), $L/14$ (427.6M), and finally $g/14$ (1.37B) in Fig. 5 (left), we study the tradeoff between knowledge accumulation and retention over time. We compare sequential fine-tuning (circles) and

269

270 *Best-in-TIME* (squares). *Best-in-TIME* scales well with model size, with larger models exhibit-
 271 ing increased affinity to merges over time. This extends and further corroborates offline merging
 272 insights by Yadav et al. (2023), who showed that model scale facilitates merging. Moreover, while
 273 Roth et al. (2024b) and Ibrahim et al. (2024) highlight better continual fine-tuning with scale, we
 274 show temporal model merging to be substantially more effective across scale. For larger models
 275 all the way to the largest ViT-g/14, *Best-in-TIME* vastly outperforms or matches sequential fine-
 276 tuning and the multitask target in knowledge retention and positive backward transfer. Furthermore,
 277 scale facilitates equivalent degrees of knowledge accumulation between sequential fine-tuning and
 278 temporal model merging. Therefore, our model scaling results strongly suggest the use of temporal
 279 model merging solutions over standard continual fine-tuning methods.

280 **Scaling the Compute.** Keeping the underlying base model fixed to ViT-B/16, we next change the
 281 available compute budget by increasing the number of update steps per task. We compare a multitask
 282 model, trained on all tasks simultaneously, to a budget-optimal *Best-in-TIME*. The only hyperpa-
 283 rameter for *Best-in-TIME* is the interpolation weight w . For each compute budget, there is a clear
 284 optimal choice of that hyperparameter (suboptimal runs shown as gray dots in Fig. 5 (right)). Higher
 285 values of w put greater emphasis on accumulation, allowing optimal accumulation-retention trade-
 286 offs to be reached at lower compute budgets. However, for a larger compute budget, less aggressive
 287 temporal model merging can achieve higher absolute trade-offs. Note that in Fig. 5 (right), we report
 288 the geometric mean between accumulation and retention, corresponding to the right-most panel in
 289 previous plots. *Best-in-TIME* scales very well across compute budgets, *clearly approaching the*
 290 *multitask upper bound* in accumulation-retention balance at larger compute budgets.

291 **Scaling the Number of Tasks.** Given that all our results until now have been with $T=20$, we next
 292 study how *Best-in-TIME* performs as we increase the number of merging time-steps to much longer
 293 time-sequences: $T=50$ and $T=100$. *Best-in-TIME* remains the optimal method of choice across
 294 different initialization and deployment strategies. Please refer to Appendix E.2 for details.

297 4 CONCLUSION

298
 299
 300 In this work, we study *temporal model merging*, addressing the chal-
 301 lenge of continually merging multi-
 302 modal models as new tasks and data
 303 arrive, and new expert models are
 304 trained in succession. To formal-
 305 ize this setting, we propose TIME,
 306 a novel unifying framework break-
 307 ing down temporal model merging
 308 into three key axes: (1) initializa-
 309 tion phase defining starting weights be-
 310 fore each task, (2) deployment phase
 311 denoting post-training expert model
 312 aggregation, and (3) the choice of
 313 merging technique. Using TIME,
 314 we conduct a large-scale systemat-
 315 ic study uncovering crucial practi-
 316 cal guidelines for temporal model
 317 merging. Our experiments on the
 318 FoMo-in-Flux benchmark spanning
 319 63 datasets, showcase that account-
 320 ing for the temporal aspect is crucial,
 321 with standard offline merging techniques falling short in this dynamic setting. Moreover, we find the
 322 particular choice of merging technique matters far less than the merging strategy for initialization
 323 and deployment. Finally, we introduce *Best-in-TIME*, which scales favorably with model size and
 outperforms existing methods for continual multimodal pretraining. Our work provides a systematic
 entry point into temporal model merging and establishes best practices for this emerging field.

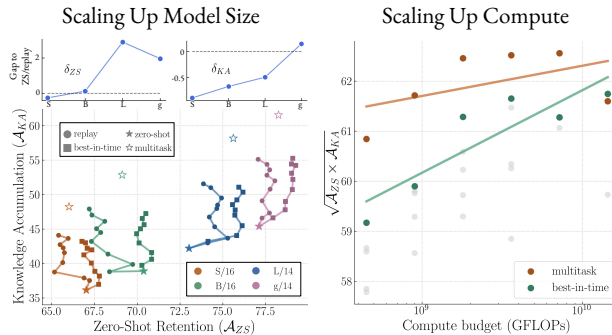


Figure 5: **Scaling up model merging.** (left) With scale, we observe continued improvements of model merging compared to the standard replay baseline. (right) Our *Best-in-TIME* method continues to improve with scaled total compute budget moving close to the multitask upper-bound. Gray points in the plot visualize suboptimal *Best-in-TIME* hyperparameter-instantiations.

324
325
326
327
328
329
330
331
332
333
334
335
336
337
338
339
340
341
342
343
344
345
346
347
348
349
350
351
352
353
354
355
356
357
358
359
360
361
362
363
364
365
366
367
368
369
370
371
372
373
374
375
376
377

REFERENCES

- Samuel Ainsworth, Jonathan Hayase, and Siddhartha Srinivasa. Git re-basin: Merging models modulo permutation symmetries. In *The Eleventh International Conference on Learning Representations*, 2023. URL <https://openreview.net/forum?id=CQsmMYmlP5T>.
- Takuya Akiba, Makoto Shing, Yujin Tang, Qi Sun, and David Ha. Evolutionary optimization of model merging recipes. *arXiv preprint arXiv:2403.13187*, 2024.
- Anton Alexandrov, Veselin Raychev, Mark Niklas Müller, Ce Zhang, Martin Vechev, and Kristina Toutanova. Mitigating catastrophic forgetting in language transfer via model merging. *arXiv preprint arXiv:2407.08699*, 2024.
- Lucas Beyer, Xiaohua Zhai, Amélie Royer, Larisa Markeeva, Rohan Anil, and Alexander Kolesnikov. Knowledge distillation: A good teacher is patient and consistent. In *Proceedings of the IEEE/CVF conference on computer vision and pattern recognition*, pp. 10925–10934, 2022.
- Jorg Bornschein, Alexandre Galashov, Ross Hemsley, Amal Rannen-Triki, Yutian Chen, Arslan Chaudhry, Xu Owen He, Arthur Douillard, Massimo Caccia, Qixuan Feng, et al. Nevis’ 22: A stream of 100 tasks sampled from 30 years of computer vision research. *JMLR*, 2023.
- Zhipeng Cai, Ozan Sener, and Vladlen Koltun. Online continual learning with natural distribution shifts: An empirical study with visual data. In *ICCV*, 2021.
- Mehdi Cherti, Romain Beaumont, Ross Wightman, Mitchell Wortsman, Gabriel Ilharco, Cade Gordon, Christoph Schuhmann, Ludwig Schmidt, and Jenia Jitsev. Reproducible scaling laws for contrastive language-image learning. *arXiv preprint arXiv:2212.07143*, 2022.
- Leshem Choshen, Elad Venezian, Shachar Don-Yehia, Noam Slonim, and Yoav Katz. Where to start? analyzing the potential value of intermediate models. *arXiv preprint arXiv:2211.00107*, 2022.
- Geoffrey Cideron, Andrea Agostinelli, Johan Ferret, Sertan Girgin, Romuald Elie, Olivier Bachem, Sarah Perrin, and Alexandre Ramé. Diversity-rewarded cfg distillation. *arXiv preprint arXiv:2410.06084*, 2024.
- MohammadReza Davari and Eugene Belilovsky. Model breadcrumbs: Scaling multi-task model merging with sparse masks. In Aleš Leonardis, Elisa Ricci, Stefan Roth, Olga Russakovsky, Torsten Sattler, and Gül Varol (eds.), *Computer Vision – ECCV 2024*, pp. 270–287, Cham, 2025. Springer Nature Switzerland. ISBN 978-3-031-73226-3.
- Pala Tej Deep, Rishabh Bhardwaj, and Soujanya Poria. Della-merging: Reducing interference in model merging through magnitude-based sampling. *arXiv preprint arXiv:2406.11617*, 2024.
- Shachar Don-Yehiya, Elad Venezian, Colin Raffel, Noam Slonim, Yoav Katz, and Leshem Choshen. Cold fusion: Collaborative descent for distributed multitask finetuning. *arXiv preprint arXiv:2212.01378*, 2022.
- Jonathan Frankle, Gintare Karolina Dziugaite, Daniel Roy, and Michael Carbin. Linear mode connectivity and the lottery ticket hypothesis. In Hal Daumé III and Aarti Singh (eds.), *Proceedings of the 37th International Conference on Machine Learning*, volume 119 of *Proceedings of Machine Learning Research*, pp. 3259–3269. PMLR, 13–18 Jul 2020. URL <https://proceedings.mlr.press/v119/frankle20a.html>.
- Saurabh Garg, Mehrdad Farajtabar, Hadi Pouransari, Raviteja Vemulapalli, Sachin Mehta, Oncel Tuzel, Vaishaal Shankar, and Fartash Faghri. Tic-clip: Continual training of clip models. In *ICLR*, 2024.
- Timur Garipov, Pavel Izmailov, Dmitrii Podoprikin, Dmitry P Vetrov, and Andrew G Wilson. Loss surfaces, mode connectivity, and fast ensembling of dnns. In S. Bengio, H. Wallach, H. Larochelle, K. Grauman, N. Cesa-Bianchi, and R. Garnett (eds.), *Advances in Neural Information Processing Systems*, volume 31. Curran Associates, Inc., 2018. URL https://proceedings.neurips.cc/paper_files/paper/2018/file/be3087e74e9100d4bc4c6268cdbe8456-Paper.pdf.

378 Charles Goddard, Shamane Siriwardhana, Malikeh Ehghaghi, Luke Meyers, Vlad Karpukhin, Brian
379 Benedict, Mark McQuade, and Jacob Solawetz. Arcee’s mergekit: A toolkit for merging large
380 language models. *arXiv preprint arXiv:2403.13257*, 2024.
381

382 Alexey Gorbатовski, Boris Shaposhnikov, Alexey Malakhov, Nikita Surnachev, Yaroslav Aksenov,
383 Ian Maksimov, Nikita Balagansky, and Daniil Gavrilov. Learn your reference model for real good
384 alignment. *arXiv preprint arXiv:2404.09656*, 2024.

385 Zhongrui Gui, Shuyang Sun, Runjia Li, Jianhao Yuan, Zhaochong An, Karsten Roth, Ameya Prabhu,
386 and Philip Torr. knn-clip: Retrieval enables training-free segmentation on continually expanding
387 large vocabularies. *arXiv preprint arXiv:2404.09447*, 2024.
388

389 Yifei He, Yuzheng Hu, Yong Lin, Tong Zhang, and Han Zhao. Localize-and-stitch: Efficient model
390 merging via sparse task arithmetic. *arXiv preprint arXiv:2408.13656*, 2024.

391 Edward J Hu, yelong shen, Phillip Wallis, Zeyuan Allen-Zhu, Yuanzhi Li, Shean Wang, Lu Wang,
392 and Weizhu Chen. LoRA: Low-rank adaptation of large language models. In *International Con-*
393 *ference on Learning Representations*, 2022. URL [https://openreview.net/forum?](https://openreview.net/forum?id=nZeVKeeFYf9)
394 [id=nZeVKeeFYf9](https://openreview.net/forum?id=nZeVKeeFYf9).
395

396 Adam Ibrahim, Benjamin Thérien, Kshitij Gupta, Mats L Richter, Quentin Anthony, Timothée
397 Lesort, Eugene Belilovsky, and Irina Rish. Simple and scalable strategies to continually pre-train
398 large language models. *arXiv preprint arXiv:2403.08763*, 2024.

399 Gabriel Ilharco, Mitchell Wortsman, Samir Yitzhak Gadre, Shuran Song, Hannaneh Hajishirzi, Si-
400 mon Kornblith, Ali Farhadi, and Ludwig Schmidt. Patching open-vocabulary models by interpo-
401 lating weights. In *NeurIPS*, 2022.
402

403 Gabriel Ilharco, Marco Tulio Ribeiro, Mitchell Wortsman, Ludwig Schmidt, Hannaneh Hajishirzi,
404 and Ali Farhadi. Editing models with task arithmetic. In *The Eleventh International Confer-*
405 *ence on Learning Representations*, 2023. URL [https://openreview.net/forum?id=](https://openreview.net/forum?id=6t0Kwf8-jrj)
406 [6t0Kwf8-jrj](https://openreview.net/forum?id=6t0Kwf8-jrj).

407 Pavel Izmailov, Dmitrii Podoprikin, Timur Garipov, Dmitry Vetrov, and Andrew Gordon Wil-
408 son. Averaging weights leads to wider optima and better generalization. *arXiv preprint*
409 *arXiv:1803.05407*, 2018.

410 Dong-Hwan Jang, Sangdoon Yun, and Dongyoon Han. Model stock: All we need is just a few
411 fine-tuned models. In *Computer Vision – ECCV 2024: 18th European Conference, Milan, Italy,*
412 *September 29–October 4, 2024, Proceedings, Part XLIV*, pp. 207–223, Berlin, Heidelberg, 2024.
413 Springer-Verlag. ISBN 978-3-031-72783-2. doi: 10.1007/978-3-031-72784-9_12. URL [https:](https://doi.org/10.1007/978-3-031-72784-9_12)
414 [//doi.org/10.1007/978-3-031-72784-9_12](https://doi.org/10.1007/978-3-031-72784-9_12).
415

416 Xisen Jin, Xiang Ren, Daniel Preotiuc-Pietro, and Pengxiang Cheng. Dataless knowledge fusion
417 by merging weights of language models. In *The Eleventh International Conference on Learning*
418 *Representations*, 2023. URL [https://openreview.net/forum?id=](https://openreview.net/forum?id=FCnohuR6AnM)
419 [FCnohuR6AnM](https://openreview.net/forum?id=FCnohuR6AnM).

420 Jean Kaddour. Stop wasting my time! saving days of imagenet and bert training with latest weight
421 averaging. *arXiv preprint arXiv:2209.14981*, 2022.

422 Siddharth Karamcheti, Suraj Nair, Ashwin Balakrishna, Percy Liang, Thomas Kollar, and Dorsa
423 Sadigh. Prismatic vlms: Investigating the design space of visually-conditioned language models.
424 *arXiv preprint arXiv:2402.07865*, 2024.

425 James Kirkpatrick, Razvan Pascanu, Neil Rabinowitz, Joel Veness, Guillaume Desjardins, Andrei A
426 Rusu, Kieran Milan, John Quan, Tiago Ramalho, Agnieszka Grabska-Barwinska, et al. Overcom-
427 ing catastrophic forgetting in neural networks. *PNAS*, 2017.
428

429 Pang Wei Koh, Shiori Sagawa, Henrik Marklund, Sang Michael Xie, Marvin Zhang, Akshay Bal-
430 subramani, Weihua Hu, Michihiro Yasunaga, Richard Lanus Phillips, Irena Gao, et al. Wilds: A
431 benchmark of in-the-wild distribution shifts. In *International conference on machine learning*,
pp. 5637–5664. PMLR, 2021.

-
- 432 Jeffrey Li, Mohammadreza Armandpour, Seyed Iman Mirzadeh, Sachin Mehta, Vaishaal Shankar,
433 Raviteja Vemulapalli, Oncel Tuzel, Mehrdad Farajtabar, Hadi Pouransari, and Fartash Faghri.
434 Tic-lm: A multi-year benchmark for continual pretraining of language models. In *NeurIPS 2024*
435 *Workshop on Scalable Continual Learning for Lifelong Foundation Models*.
- 436 Margaret Li, Suchin Gururangan, Tim Dettmers, Mike Lewis, Tim Althoff, Noah A Smith, and Luke
437 Zettlemoyer. Branch-train-merge: Embarrassingly parallel training of expert language models.
438 *arXiv preprint arXiv:2208.03306*, 2022.
- 439 Tao Li, Weisen Jiang, Fanghui Liu, Xiaolin Huang, and James T Kwok. Learning scalable model
440 soup on a single gpu: An efficient subspace training strategy. *arXiv preprint arXiv:2407.03641*,
441 2024.
- 442 Yong Lin, Hangyu Lin, Wei Xiong, Shizhe Diao, Jianmeng Liu, Jipeng Zhang, Rui Pan, Haoxiang
443 Wang, Wenbin Hu, Hanning Zhang, Hanze Dong, Renjie Pi, Han Zhao, Nan Jiang, Heng Ji, Yuan
444 Yao, and Tong Zhang. Mitigating the alignment tax of RLHF. In Yaser Al-Onaizan, Mohit Bansal,
445 and Yun-Nung Chen (eds.), *Proceedings of the 2024 Conference on Empirical Methods in Natural*
446 *Language Processing*, pp. 580–606, Miami, Florida, USA, November 2024. Association for Com-
447 putational Linguistics. URL <https://aclanthology.org/2024.emnlp-main.35>.
- 448 Zhiqiu Lin, Jia Shi, Deepak Pathak, and Deva Ramanan. The clear benchmark: Continual learning
449 on real-world imagery. In *NeurIPS*, 2021.
- 450 Adam Liska, Tomas Kocisky, Elena Gribovskaya, Tayfun Terzi, Eren Sezener, Devang Agrawal,
451 D’Autume Cyprien De Masson, Tim Scholtes, Manzil Zaheer, Susannah Young, et al. Stream-
452 ingqa: A benchmark for adaptation to new knowledge over time in question answering models.
453 In *International Conference on Machine Learning*, pp. 13604–13622. PMLR, 2022.
- 454 Tianlin Liu, Shangmin Guo, Leonardo Bianco, Daniele Calandriello, Quentin Berthet, Felipe
455 Linares-López, Jessica Hoffmann, Lucas Dixon, Michal Valko, and Mathieu Blondel. Decoding-
456 time realignment of language models. In Ruslan Salakhutdinov, Zico Kolter, Katherine Heller,
457 Adrian Weller, Nuria Oliver, Jonathan Scarlett, and Felix Berkenkamp (eds.), *Proceedings*
458 *of the 41st International Conference on Machine Learning*, volume 235 of *Proceedings of*
459 *Machine Learning Research*, pp. 31015–31031. PMLR, 21–27 Jul 2024. URL [https://](https://proceedings.mlr.press/v235/liu24r.html)
460 proceedings.mlr.press/v235/liu24r.html.
- 461 Ilya Loshchilov and Frank Hutter. Decoupled weight decay regularization. *arXiv preprint*
462 *arXiv:1711.05101*, 2017.
- 463 Jinliang Lu, Ziliang Pang, Min Xiao, Yaochen Zhu, Rui Xia, and Jiajun Zhang. Merge, ensemble,
464 and cooperate! a survey on collaborative strategies in the era of large language models. *arXiv*
465 *preprint arXiv:2407.06089*, 2024.
- 466 Daniel Marczak, Bartłomiej Twardowski, Tomasz Trzciniński, and Sebastian Cygert. Magmax: Lever-
467 aging model merging for seamless continual learning. *arXiv preprint arXiv:2407.06322*, 2024.
- 468 Michael S Matena and Colin Raffel. Merging models with fisher-weighted averaging. In Alice H.
469 Oh, Alekh Agarwal, Danielle Belgrave, and Kyunghyun Cho (eds.), *Advances in Neural Infor-*
470 *mation Processing Systems*, 2022. URL [https://openreview.net/forum?id=LSKlp_](https://openreview.net/forum?id=LSKlp_aceOC)
471 [aceOC](https://openreview.net/forum?id=LSKlp_aceOC).
- 472 Matías Mendieta, Boran Han, Xingjian Shi, Yi Zhu, and Chen Chen. Towards geospatial foundation
473 models via continual pretraining. In *Proceedings of the IEEE/CVF International Conference on*
474 *Computer Vision*, pp. 16806–16816, 2023.
- 475 Sachit Menon and Carl Vondrick. Visual classification via description from large language models.
476 In *The Eleventh International Conference on Learning Representations*, 2023. URL [https://](https://openreview.net/forum?id=j1AjNL8z5cs)
477 openreview.net/forum?id=j1AjNL8z5cs.
- 478 Remi Munos, Michal Valko, Daniele Calandriello, Mohammad Gheshlaghi Azar, Mark Rowland,
479 Zhaohan Daniel Guo, Yunhao Tang, Matthieu Geist, Thomas Mesnard, Côme Fiegl, Andrea
480 Michi, Marco Selvi, Sertan Girgin, Nikola Momchev, Olivier Bachem, Daniel J Mankowitz,
481 Doina Precup, and Bilal Piot. Nash learning from human feedback. In Ruslan Salakhutdinov, Zico

486 Kolter, Katherine Heller, Adrian Weller, Nuria Oliver, Jonathan Scarlett, and Felix Berkenkamp
487 (eds.), *Proceedings of the 41st International Conference on Machine Learning*, volume 235 of
488 *Proceedings of Machine Learning Research*, pp. 36743–36768. PMLR, 21–27 Jul 2024. URL
489 <https://proceedings.mlr.press/v235/munos24a.html>.
490

491 Anshul Nasery, Jonathan Hayase, Pang Wei Koh, and Sewoong Oh. Pleas–merging models with
492 permutations and least squares. *arXiv preprint arXiv:2407.02447*, 2024.

493 Behnam Neyshabur, Hanie Sedghi, and Chiyuan Zhang. What is being transferred in transfer learn-
494 ing? In H. Larochelle, M. Ranzato, R. Hadsell, M.F. Balcan, and H. Lin (eds.), *Advances*
495 *in Neural Information Processing Systems*, volume 33, pp. 512–523. Curran Associates, Inc.,
496 2020. URL [https://proceedings.neurips.cc/paper_files/paper/2020/](https://proceedings.neurips.cc/paper_files/paper/2020/file/0607f4c705595b911a4f3e7a127b44e0-Paper.pdf)
497 [file/0607f4c705595b911a4f3e7a127b44e0-Paper.pdf](https://proceedings.neurips.cc/paper_files/paper/2020/file/0607f4c705595b911a4f3e7a127b44e0-Paper.pdf).
498

499 Kai Nylund, Suchin Gururangan, and Noah A Smith. Time is encoded in the weights of finetuned
500 language models. *arXiv preprint arXiv:2312.13401*, 2023.

501 Changdae Oh, Yixuan Li, Kyungwoo Song, Sangdoon Yun, and Dongyoon Han. Dawin: Training-
502 free dynamic weight interpolation for robust adaptation. *arXiv preprint arXiv:2410.03782*, 2024.
503

504 Oleksiy Ostapenko, Timothee Lesort, Pau Rodríguez, Md Rifat Arefin, Arthur Douillard, Irina Rish,
505 and Laurent Charlin. Continual learning with foundation models: An empirical study of latent
506 replay. In *Conference on Lifelong Learning Agents (CoLLAs)*, 2022.

507 Jyothish Pari, Samy Jelassi, and Pulkit Agrawal. Collective model intelligence requires compatible
508 specialization. *arXiv preprint arXiv:2411.02207*, 2024.
509

510 Adam Paszke, Sam Gross, Francisco Massa, Adam Lerer, James Bradbury, Gregory Chanan, Trevor
511 Killeen, Zeming Lin, Natalia Gimelshein, Luca Antiga, et al. Pytorch: An imperative style, high-
512 performance deep learning library. *Advances in neural information processing systems*, 32, 2019.
513

514 Ameya Prabhu, Zhipeng Cai, Puneet Dokania, Philip Torr, Vladlen Koltun, and Ozan Sener. Online
515 continual learning without the storage constraint. *arXiv preprint arXiv:2305.09253*, 2023a.

516 Ameya Prabhu, Hasan Abed Al Kader Hammoud, Puneet Dokania, Philip HS Torr, Ser-Nam Lim,
517 Bernard Ghanem, and Adel Bibi. Computationally budgeted continual learning: What does mat-
518 ter? In *CVPR*, 2023b.

519 Ameya Prabhu, Hasan Abed Al Kader Hammoud, Ser-Nam Lim, Bernard Ghanem, Philip HS Torr,
520 and Adel Bibi. From categories to classifier: Name-only continual learning by exploring the web.
521 *arXiv preprint arXiv:2311.11293*, 2023c.
522

523 Sarah Pratt, Ian Covert, Rosanne Liu, and Ali Farhadi. What does a platypus look like? gener-
524 ating customized prompts for zero-shot image classification. In *Proceedings of the IEEE/CVF*
525 *International Conference on Computer Vision (ICCV)*, pp. 15691–15701, October 2023.
526

527 Alec Radford, Jong Wook Kim, Chris Hallacy, Aditya Ramesh, Gabriel Goh, Sandhini Agarwal,
528 Girish Sastry, Amanda Askell, Pamela Mishkin, Jack Clark, et al. Learning transferable visual
529 models from natural language supervision. In *International conference on machine learning*, pp.
530 8748–8763. PMLR, 2021.

531 Alexandre Rame, Kartik Ahuja, Jianyu Zhang, Matthieu Cord, Leon Bottou, and David Lopez-Paz.
532 Model ratatouille: Recycling diverse models for out-of-distribution generalization. In Andreas
533 Krause, Emma Brunskill, Kyunghyun Cho, Barbara Engelhardt, Sivan Sabato, and Jonathan Scar-
534 lett (eds.), *Proceedings of the 40th International Conference on Machine Learning*, volume 202
535 of *Proceedings of Machine Learning Research*, pp. 28656–28679. PMLR, 23–29 Jul 2023. URL
536 <https://proceedings.mlr.press/v202/rame23a.html>.
537

538 Alexandre Ramé, Johan Ferret, Nino Vieillard, Robert Dadashi, Léonard Hussenot, Pierre-Louis
539 Cedoz, Pier Giuseppe Sessa, Sertan Girgin, Arthur Douillard, and Olivier Bachem. Warp: On the
benefits of weight averaged rewarded policies. *arXiv preprint arXiv:2406.16768*, 2024.

540 Alexandre Ramé, Matthieu Kirchmeyer, Thibaud Rahier, Alain Rakotomamonjy, Patrick Gallinari,
541 and Matthieu Cord. Diverse weight averaging for out-of-distribution generalization. In *Proceed-*
542 *ings of the 36th International Conference on Neural Information Processing Systems, NIPS '22,*
543 2024. ISBN 9781713871088.

544 Alexandre Ramé, Nino Vieillard, Léonard Hussenot, Robert Dadashi, Geoffrey Cideron, Olivier
545 Bachem, and Johan Ferret. Warm: On the benefits of weight averaged reward models. *arXiv*
546 *preprint arXiv:2401.12187*, 2024.

548 Regent’s, ParkLondon, Ukj, and . Utans. Weight averaging for neural networksand local resampling.
549 1996. URL <https://api.semanticscholar.org/CorpusID:475398>.

550 Mark Rofin, Nikita Balagansky, and Daniil Gavrilov. Linear interpolation in parameter space is good
551 enough for fine-tuned language models. *arXiv preprint arXiv:2211.12092*, 2022.

553 Karsten Roth, Lukas Thede, A. Sophia Koepke, Oriol Vinyals, Olivier J Henaff, and Zeynep Akata.
554 Fantastic gains and where to find them: On the existence and prospect of general knowledge
555 transfer between any pretrained model. In *The Twelfth International Conference on Learning*
556 *Representations*, 2024a. URL <https://openreview.net/forum?id=m50eKHcTtz>.

558 Karsten Roth, Vishaal Udandaraao, Sebastian Dziadzio, Ameya Prabhu, Mehdi Cherti, Oriol Vinyals,
559 Olivier Hénaff, Samuel Albanie, Matthias Bethge, and Zeynep Akata. A practitioner’s guide to
560 continual multimodal pretraining. *arXiv preprint arXiv:2408.14471*, 2024b.

561 Sunny Sanyal, Atula Tejaswi Neerkaje, Jean Kaddour, Abhishek Kumar, and sujay sanghavi. Early
562 weight averaging meets high learning rates for LLM pre-training. In *First Conference on Lan-*
563 *guage Modeling*, 2024. URL <https://openreview.net/forum?id=IA8CWtNkUr>.

565 Christoph Schuhmann, Romain Beaumont, Richard Vencu, Cade Gordon, Ross Wightman, Mehdi
566 Cherti, Theo Coombes, Aarush Katta, Clayton Mullis, Mitchell Wortsman, et al. Laion-5b: An
567 open large-scale dataset for training next generation image-text models. *Advances in Neural*
568 *Information Processing Systems*, 35:25278–25294, 2022.

569 Ekansh Sharma, Daniel M Roy, and Gintare Karolina Dziugaite. The non-local model merging
570 problem: Permutation symmetries and variance collapse. *arXiv preprint arXiv:2410.12766*, 2024.

572 Li Shen, Anke Tang, Enneng Yang, Guibing Guo, Yong Luo, Lefei Zhang, Xiaochun Cao, Bo Du,
573 and Dacheng Tao. Efficient and effective weight-ensembling mixture of experts for multi-task
574 model merging. *arXiv preprint arXiv:2410.21804*, 2024.

575 Ken Shoemake. Animating rotation with quaternion curves. *Proceedings of the 12th annual*
576 *conference on Computer graphics and interactive techniques*, 1985. URL <https://api.semanticscholar.org/CorpusID:11290566>.

578 Shikhar Srivastava, Md Yousuf Harun, Robik Shrestha, and Christopher Kanan. Improving multi-
579 modal large language models using continual learning. *arXiv preprint arXiv:2410.19925*, 2024.

581 George Stoica, Pratik Ramesh, Boglarka Ecsedi, Leshem Choshen, and Judy Hoffman. Model
582 merging with svd to tie the knots. *arXiv preprint arXiv:2410.19735*, 2024.

584 Zafir Stojanovski, Karsten Roth, and Zeynep Akata. Momentum-based weight interpolation of
585 strong zero-shot models for continual learning. *arXiv preprint arXiv:2211.03186*, 2022.

586 Yi-Lin Sung, Linjie Li, Kevin Lin, Zhe Gan, Mohit Bansal, and Lijuan Wang. An empirical study
587 of multimodal model merging. *arXiv preprint arXiv:2304.14933*, 2023.

589 Derek Tam, Mohit Bansal, and Colin Raffel. Merging by matching models in task parameter
590 subspaces. *Transactions on Machine Learning Research*, 2024a. ISSN 2835-8856. URL
591 <https://openreview.net/forum?id=qNGo6ghWFB>.

592 Derek Tam, Yash Kant, Brian Lester, Igor Gilitschenski, and Colin Raffel. Realistic evaluation of
593 model merging for compositional generalization. *arXiv preprint arXiv:2409.18314*, 2024b.

-
- 594 Lukas Thede, Karsten Roth, Olivier J Hénaff, Matthias Bethge, and Zeynep Akata. Reflect-
595 ing on the state of rehearsal-free continual learning with pretrained models. *arXiv preprint*
596 *arXiv:2406.09384*, 2024.
597
- 598 Ke Wang, Nikolaos Dimitriadis, Alessandro Favero, Guillermo Ortiz-Jimenez, Francois Fleuret,
599 and Pascal Frossard. Lines: Post-training layer scaling prevents forgetting and enhances model
600 merging. *arXiv preprint arXiv:2410.17146*, 2024a.
- 601 Ke Wang, Nikolaos Dimitriadis, Guillermo Ortiz-Jimenez, François Fleuret, and Pascal Frossard.
602 Localizing task information for improved model merging and compression. *arXiv preprint*
603 *arXiv:2405.07813*, 2024b.
604
- 605 Mitchell Wortsman, Gabriel Ilharco, Samir Ya Gadre, Rebecca Roelofs, Raphael Gontijo-Lopes,
606 Ari S Morcos, Hongseok Namkoong, Ali Farhadi, Yair Carmon, Simon Kornblith, and Lud-
607 wig Schmidt. Model soups: averaging weights of multiple fine-tuned models improves accu-
608 racy without increasing inference time. In Kamalika Chaudhuri, Stefanie Jegelka, Le Song,
609 Csaba Szepesvari, Gang Niu, and Sivan Sabato (eds.), *Proceedings of the 39th International*
610 *Conference on Machine Learning*, volume 162 of *Proceedings of Machine Learning Research*,
611 pp. 23965–23998. PMLR, 17–23 Jul 2022a. URL <https://proceedings.mlr.press/v162/wortsman22a.html>.
612
- 613 Mitchell Wortsman, Gabriel Ilharco, Jong Wook Kim, Mike Li, Simon Kornblith, Rebecca Roelofs,
614 Raphael Gontijo Lopes, Hannaneh Hajishirzi, Ali Farhadi, Hongseok Namkoong, and Ludwig
615 Schmidt. Robust fine-tuning of zero-shot models. In *Proceedings of the IEEE/CVF Conference*
616 *on Computer Vision and Pattern Recognition (CVPR)*, pp. 7959–7971, June 2022b.
- 617 Feng Xiong, Runxi Cheng, Wang Chen, Zhanqiu Zhang, Yiwen Guo, Chun Yuan, and Ruifeng
618 Xu. Multi-task model merging via adaptive weight disentanglement. *arXiv preprint*
619 *arXiv:2411.18729*, 2024.
620
- 621 Prateek Yadav, Derek Tam, Leshem Choshen, Colin Raffel, and Mohit Bansal. TIES-merging: Re-
622 solving interference when merging models. In *Thirty-seventh Conference on Neural Information*
623 *Processing Systems*, 2023. URL <https://openreview.net/forum?id=xtaX3WyCj1>.
624
- 625 Prateek Yadav, Colin Raffel, Mohammed Muqeeth, Lucas Caccia, Haokun Liu, Tianlong Chen,
626 Mohit Bansal, Leshem Choshen, and Alessandro Sordani. A survey on model moerging:
627 Recycling and routing among specialized experts for collaborative learning. *arXiv preprint*
628 *arXiv:2408.07057*, 2024a.
- 629 Prateek Yadav, Tu Vu, Jonathan Lai, Alexandra Chronopoulou, Manaal Faruqui, Mohit Bansal,
630 and Tsendsuren Munkhdalai. What matters for model merging at scale? *arXiv preprint*
631 *arXiv:2410.03617*, 2024b.
- 632 Enneng Yang, Li Shen, Guibing Guo, Xingwei Wang, Xiaochun Cao, Jie Zhang, and Dacheng Tao.
633 Model merging in llms, mllms, and beyond: Methods, theories, applications and opportunities.
634 *arXiv preprint arXiv:2408.07666*, 2024a.
635
- 636 Enneng Yang, Li Shen, Zhenyi Wang, Guibing Guo, Xiaojun Chen, Xingwei Wang, and Dacheng
637 Tao. Representation surgery for multi-task model merging. *arXiv preprint arXiv:2402.02705*,
638 2024b.
- 639 Çağatay Yıldız, Nishaanth Kanna Ravichandran, Prishruit Punia, Matthias Bethge, and Beyza Ermis.
640 Investigating continual pretraining in large language models: Insights and implications. *arXiv*
641 *preprint arXiv:2402.17400*, 2024.
642
- 643 Le Yu, Bowen Yu, Haiyang Yu, Fei Huang, and Yongbin Li. Language models are super mario:
644 Absorbing abilities from homologous models as a free lunch. In Ruslan Salakhutdinov, Zico
645 Kolter, Katherine Heller, Adrian Weller, Nuria Oliver, Jonathan Scarlett, and Felix Berkenkamp
646 (eds.), *Proceedings of the 41st International Conference on Machine Learning*, volume 235 of
647 *Proceedings of Machine Learning Research*, pp. 57755–57775. PMLR, 21–27 Jul 2024. URL
<https://proceedings.mlr.press/v235/yu24p.html>.

648 Kerem Zaman, Leshem Choshen, and Shashank Srivastava. Fuse to forget: Bias reduction and
649 selective memorization through model fusion. *arXiv preprint arXiv:2311.07682*, 2023.
650

651 Friedemann Zenke, Ben Poole, and Surya Ganguli. Continual learning through synaptic intelligence.
652 In *ICML*, 2017.

653 Renrui Zhang, Rongyao Fang, Peng Gao, Wei Zhang, Kunchang Li, Jifeng Dai, Yu Qiao, and Hong-
654 sheng Li. Tip-adapter: Training-free clip-adapter for better vision-language modeling. *arXiv*
655 *preprint arXiv:2111.03930*, 2021.
656

657 Shenghe Zheng and Hongzhi Wang. Free-merging: Fourier transform for model merging with
658 lightweight experts. *arXiv preprint arXiv:2411.16815*, 2024.

659 Luca Zhou, Daniele Solombrino, Donato Crisostomi, Maria Sofia Bucarelli, Fabrizio Silvestri, and
660 Emanuele Rodolà. Atm: Improving model merging by alternating tuning and merging. *arXiv*
661 *preprint arXiv:2411.03055*, 2024.
662
663
664
665
666
667
668
669
670
671
672
673
674
675
676
677
678
679
680
681
682
683
684
685
686
687
688
689
690
691
692
693
694
695
696
697
698
699
700
701

Acknowledgements. The authors would like to thank (in random order) Shyamgopal Karthik, Shashwat Goel, Ankit Sonthalia, Olivier Hénaff, Alexandre Ramé, and Daniel Marczak for helpful feedback. The plotting style in our work is inspired by figures from Beyer et al. (2022). The style of Fig. 2 is inspired by Figure 1 of Karamcheti et al. (2024). VU, KR, and SD thank the International Max Planck Research School for Intelligent Systems (IMPRS-IS). VU, KR, and SD also thank the European Laboratory for Learning and Intelligent Systems (ELLIS) PhD program for support. VU is supported by a Google PhD Fellowship in Machine Intelligence. SA is supported by a Newton Trust Grant. AP is supported by the Federal Ministry of Education and Research (BMBF), FKZ: 011524085B. MB acknowledges financial support via the Open Philanthropy Foundation funded by the Good Ventures Foundation. MB is a member of the Machine Learning Cluster of Excellence, funded by the Deutsche Forschungsgemeinschaft (DFG, German Research Foundation) under Germany’s Excellence Strategy – EXC number 2064/1 – Project number 390727645. ZA acknowledges the support from the German Research Foundation (DFG): SFB 1233, Robust Vision: Inference Principles and Neural Mechanisms, project number: 276693517 and ERC Grant DEXIM, project number: 853489. This research utilized compute resources at the Tübingen Machine Learning Cloud, DFG FKZ INST 37/1057-1 FUGG.

A RELATED WORKS

Model Merging. We provide a short overview of the model merging literature, detailed in these excellent surveys (Yadav et al., 2024a; Yang et al., 2024a). While both model aggregation through distillation Roth et al. (2024a); Cideron et al. (2024) and averaging checkpoints during training (Kaddour, 2022; Sanyal et al., 2024; Li et al., 2024) have shown success, the requirement of additional compute limits practicability of these methods (Prabhu et al., 2023b). Instead, recent work (Wortsman et al., 2022b;a; Ilharco et al., 2022; 2023; Rame et al., 2023; Sanyal et al., 2024; Sung et al., 2023; Pari et al., 2024; Nylund et al., 2023; Zaman et al., 2023; Stoica et al., 2024; Wang et al., 2024b; He et al., 2024; Oh et al., 2024; Shen et al., 2024; Sharma et al., 2024; Goddard et al., 2024; Yadav et al., 2024a; Xiong et al., 2024; Yang et al., 2024b; Lu et al., 2024; Zheng & Wang, 2024; Nasery et al., 2024) has shown the effectiveness of training-free weight averaging and interpolation of fine-tuned expert models to produce an improved base model, benefiting from (linear) mode connectivity in models fine-tuned from a single pre-trained checkpoint Izmailov et al. (2018); Ramé et al. (2024); Neyshabur et al. (2020); Frankle et al. (2020); Ainsworth et al. (2023). These insights have been extended into weight-averaged reward models Ramé et al. (2024), policy models Ramé et al. (2024) with spherical interpolation, and KL-constrained RLHF Lin et al. (2024); Liu et al. (2024); Munos et al. (2024); Gorbатовski et al. (2024). Works such as Fisher-Merge Matena & Raffel (2022), TIES Yadav et al. (2023), RegMean Jin et al. (2023), MATS Tam et al. (2024a), DELLA Deep et al. (2024), DARE Yu et al. (2024), Breadcrumbs Davari & Belilovsky (2025), evolutionary merging Akiba et al. (2024) and MagMax Marczak et al. (2024) have explored merging strategies beyond simple interpolation to determine which weights should be merged across expert models. These methods have different benefits for in- and out-of-distribution generalization across domains Tam et al. (2024b), though recently they have been shown to perform similarly at scale Yadav et al. (2024b). Additionally, some works have explored the initialization dimension for effectively merging models (Choshen et al., 2022; Don-Yehiya et al., 2022; Zhou et al., 2024; Marczak et al., 2024). In this work, we propose a unifying framework for temporal merging and conduct the most comprehensive study of this topic to date.

Continual Pretraining extends beyond standard Continual Learning (Prabhu et al., 2023a; Roth et al., 2024b), focusing on large-scale model updates starting from pretrained foundation models Ibrahim et al. (2024); Garg et al. (2024); Roth et al. (2024b); Gui et al. (2024); Prabhu et al. (2023c) and addressing more complex and substantial update tasks Lin et al. (2021); Cai et al. (2021); Liska et al. (2022); Garg et al. (2024); Bornschein et al. (2023); Roth et al. (2024b). There has been limited exploration into using model merging for continual pretraining (Marczak et al., 2024; Alexandrov et al., 2024; Stojanovski et al., 2022; Roth et al., 2024b), as most prior works focus on training strategies including regularization objectives and learning-rate schedules (Roth et al., 2024b; Prabhu et al., 2023b; Garg et al., 2024; Ibrahim et al., 2024; Srivastava et al., 2024; Li et al.; Yıldız et al., 2024; Thede et al., 2024; Ostapenko et al., 2022; Mendieta et al., 2023). We keep the training strategy fixed, and provide an in-depth exploration beyond simple merging techniques.

B DETAILS OF THE MERGING METHODS

Denoting the number of models to merge at timestep t as M_t (with $t = 0$ and $M_t = M$ for standard model merging), we can define these methods as follows:

Weight Averaging Regent et al. (1996); Wortsman et al. (2022b); Ilharco et al. (2022); Stojanovski et al. (2022); Roth et al. (2024b) simply employs a uniformly weighted, element-wise average over all models $\theta_{t,i}$, resulting in a merge function $f_{\text{merge}}^{\text{WA}}$:

$$\theta_t = \frac{1}{M_t} \sum_i \theta_{t,i}. \quad (2)$$

SLERP Shoemake (1985); Ramé et al. (2024) assumes weights to live on a hypersphere, and consequently conducts interpolation along a curved path connecting weight entries. In particular, for two models $\theta_{t,1}$ and $\theta_{t,2}$ deriving from some base weight θ_{t-1} and the corresponding task vectors $\delta_{t,i} = \theta_{t,i} - \theta_{t-1}$, SLERP with interpolation weight λ is defined as

$$\theta_t = \theta_{t-1} + \frac{\sin(1-\lambda)\Omega_{1,2}}{\sin\Omega_{1,2}} \cdot \delta_{t,1} + \frac{\sin\lambda\Omega_{1,2}}{\sin\Omega_{1,2}} \cdot \delta_{t,2} \quad (3)$$

with $\Omega_{1,2}$ being the angle between task vectors $\delta_{t,1}$ and $\delta_{t,2}$. We denote the corresponding merge function $f_{\text{merge}}^{\text{SLERP}}$.

Task Arithmetic Ilharco et al. (2023) defines the merge as a function over task vectors $\delta_{t,i} = \theta_{t,i} - \theta_{t-1}$ for each weight $\theta_{t,i}$ fine-tuned from θ_{t-1} . This introduces a simple merge formalism $f_{\text{merge}}^{\text{TA}}$ for weighted parameter averaging with a scale λ :

$$\theta_t = \theta_{t-1} + \lambda \frac{1}{M_t} \sum_i \delta_{t,i} \quad (4)$$

TIES Yadav et al. (2023) builds on the task arithmetic formalism through controlled pruning of task vector entries with low magnitude. Moreover, the sign for each final merged parameter is set based on the sign of the highest total magnitude across the merge candidates. The final update follows basic task arithmetic, only for entries with matching signs. We refer to the respective merge function as $f_{\text{merge}}^{\text{TIES}}$.

DARE Yu et al. (2024) is a similar extension of task arithmetic, but instead of targeted pruning, it randomly zeroes out task vector entries using a random mask $Z_i \sim \text{Bernoulli}(p)$ and masking probability p . Final task vector values for $f_{\text{merge}}^{\text{DARE}}$ are then rescaled based on p :

$$\delta_{t,i}^{\text{DARE}} = \frac{(1 - Z_i)\delta_{t,i}}{1 - p}. \quad (5)$$

Model Stock Jang et al. (2024) provides a geometric extension of simple weight averaging as done in Model Soup Wortsman et al. (2022a) by incorporating base weights θ_{t-1} into the merging process. Given fine-tuned weights $\theta_{t,1}$ and $\theta_{t,2}$, the Model Stock merge $f_{\text{merge}}^{\text{Stock}}$ is defined as follows:

$$\theta_t = \frac{2 \cdot \cos\Omega_{1,2}}{1 + \Omega_{1,2}} \cdot (\theta_{t,2} - \theta_{t,1}) + \left(1 - \frac{2 \cdot \cos\Omega_{1,2}}{1 + \cos\Omega_{1,2}}\right), \quad (6)$$

utilizing angle $\Omega_{1,2}$ between task vectors $\delta_{t,1}$ and $\delta_{t,2}$.

Breadcrumbs Davari & Belilovsky (2025) deploys another variation on task arithmetic for model merging. In particular, for a given task vector $\delta_{t,i}$, extreme left and right tails of the absolute magnitude distribution in $\delta_{t,i}$ are zeroed out with left and right thresholds β and γ . The modified task vectors $\delta_{t,i}^{\text{Bread}}$ are then applied on base weights θ_{t-1} following the task arithmetic setup, and giving $f_{\text{merge}}^{\text{Bread}}$.

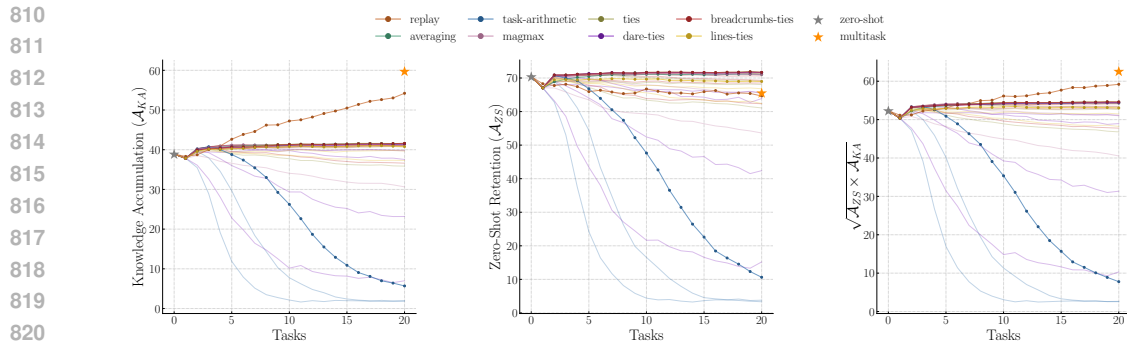


Figure 6: **Offline merging methods struggle with TIME.** All tested merging techniques perform extremely poorly, and are unable to adapt to the temporal setting, underperforming even a simple **replay** baseline that sequentially trains the base model on task-replayed data.

MagMax Marczak et al. (2024) also uses task vectors—given multiple task vectors $\delta_{t,i}$ (with increments possible along both time t and count axis i), the final task vector δ_t is yielded through maximum magnitude entry selection; copying the largest magnitude entries across all $\{\delta_{t,i}\}$ into δ_t , giving $f_{\text{merge}}^{\text{Max}}$.

LiNeS Wang et al. (2024a), for **L**ayer-increasing **N**etwork **S**caling, scales weight updates based on their respective layer depth enabling early layers to remain close to original pretraining weights (cf. Neyshabur et al. (2020)). Given task vectors $\delta_{t,i}$, now broken down across model layers $\delta_{t,i}^l$ with $l \in [1, \dots, L]$ and L the number of layers, LiNeS follows the base task arithmetic merging formalism, but updates task vectors as

$$\delta_{t,i}^{\text{LiNeS}} = \text{concat}(\lambda^{l=1} \delta_{t,i}^{l=1}, \dots, \lambda^{l=L} \delta_{t,i}^{l=L}) \quad (7)$$

with layer-scaled interpolation weights $\lambda^l = \alpha + \beta \frac{l-1}{L-1}$ and hyperparameters α, β , giving $f_{\text{merge}}^{\text{Lines}}$.

C PLOTTING STYLE

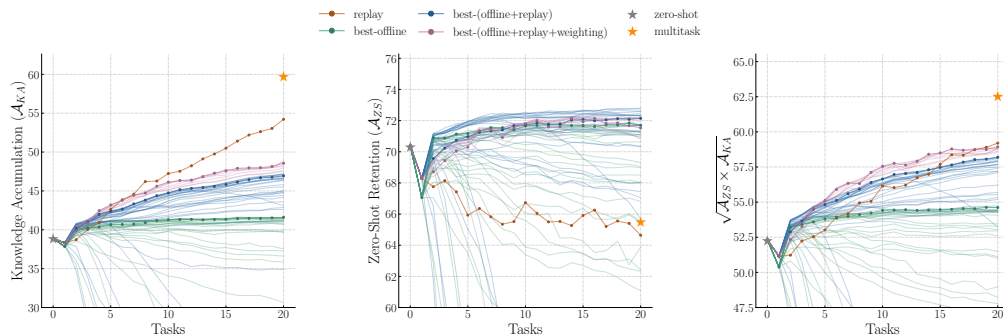
Across TIME, we utilize a common plotting style to visualize our results—with three base subplots (see for e.g., Fig. 5):

- Knowledge Accumulation (\mathcal{A}_{KA}) versus number of tasks over time. In this plot, a gray star indicates the base-weight zero-shot performance on adaptation datasets. An orange star indicates an upper bound achieved through jointly training on all the data at once, with no separation over time.
- Zero-Shot Retention (\mathcal{A}_{ZS}) versus number of tasks over time. Similar to \mathcal{A}_{KA} versus tasks, this plot visualizes merging results for TIME-variants, but measuring performance on withheld evaluation datasets. Again, gray and orange star indicate base and joint training lower and upper bounds, respectively.
- Finally, we also aggregate both previous plots into one showcasing the progression of merged performance geometric mean $\sqrt{\mathcal{A}_{ZS} \times \mathcal{A}_{KA}}$ over time; utilizing the same star indication as in the previous subplots.

The only deviation from this plotting style is Fig. 5. The left panel visualizes the trajectory across tasks in the \mathcal{A}_{KA} - \mathcal{A}_{ZS} space. Here, full-colored stars reference base model performance and hollow stars the corresponding joint training upper bounds. The right panel shows the geometric mean of \mathcal{A}_{KA} and \mathcal{A}_{ZS} at the end of the last task for different compute budgets.

Finally, several plots such as Figs. 4, 6 and 7 show the extensive scale of our experiments through background visualizations of sub-optimal hyperparameter choices in lighter colors (as opposed to the optimal choices using darker coloring). This plotting style is loosely inspired by Beyer et al. (2022).

864
865
866
867
868
869
870
871
872
873
874



875 **Figure 7: Improving offline merging.** We identify two simple methods for adapting offline-merging
876 methods to the temporal setting: (1) replaying data from previous tasks (**best-(offline+replay)**) and
877 (2) recency-biased weighting of task checkpoints (**best-(offline+replay+weighting)**). With these
878 method improvements, offline merging methods can match the **replay** baseline.

880 D ADDITIONAL OFFLINE MERGING EXPERIMENTS

881 D.1 REPLAY AND TIME-WEIGHTING

882
883 In this section, we analyze extensions to offline methods that can help close the gap to the replay
884 baseline. As the continual fine-tuning baseline *replays* on past data from all previous tasks while
885 training at the current task t , can this task data-mixing also help offline merging methods?
886
887

888 **Data replaying improves offline merging.** Since offline methods operate entirely under a task-
889 independent assumption, they fail to capture any temporal dependencies. Fig. 7 shows that simply
890 applying data-replay on top of standard offline merging leads to significant boosts in the overall
891 performance. For instance, **best-(offline+replay)** achieves 58.2% compared to **best-offline** at 54.6%,
892 bringing it closer to the **replay** baseline. However, a notable performance gap remains, with **best-**
893 **(offline+replay)** at 58.2% falling short of **replay** at 59.1%.

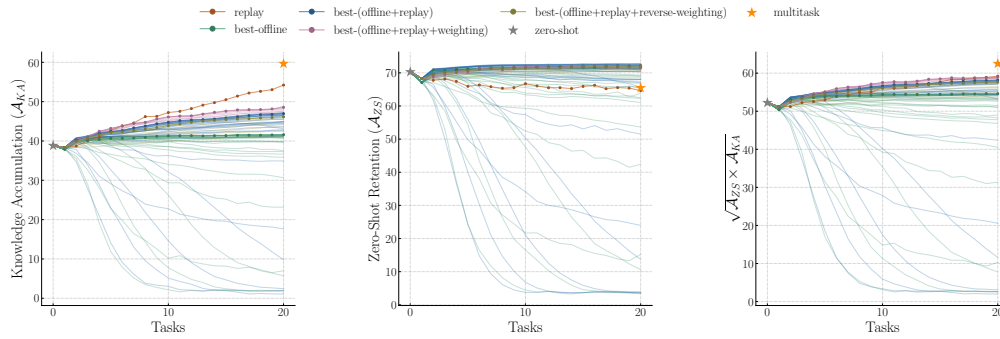
894 **Recency-biased weighting helps.** Next, unlike in standard *offline* averaging, where all task check-
895 points are weighted uniformly, we impose temporal ordering via non-uniform weighting for offline
896 merging. We explore several recency-biased, non-uniform weighting schemes, assigning higher
897 weights to more recent tasks to account for the temporal nature of the setting.

898 We explore various discounting schemes: logarithmic, quadratic, exponential, and cubic, applied
899 to the best offline merge replay method from the previous experiment (please refer to the sup-
900 plementary for details). As shown in Fig. 7, these schemes improve performance, with **best-**
901 **(offline+replay+weighting)** reaching 58.9%, yet still falling slightly short of the **replay** baseline at
902 58.9%. These results provide strong evidence that accounting for the new temporal axis is crucial
903 for effective temporal model merging, even when implemented as an extension of offline merging.
904 **Key takeaway:** accounting for the time aspect is crucial for effective temporal model merging, even
905 as an extension on top of standard offline merging. Still, a small gap to the simple replay baseline
906 remains.

908 D.2 REVERSED NON-UNIFORM WEIGHTING SCHEMES

909
910 In Fig. 7, we found that a simple yet effective method for boosting the performance of offline merg-
911 ing methods is recency-biased non-uniform weighting, i.e. giving larger weights to more recent
912 checkpoints while merging. Here, we ask the question—what if we reversed the weighting schemes
913 such that we give larger weights to older task checkpoints? From Fig. 8, we indeed observe that
914 such a reverse strategy performs worse than the best recency-biased weighting schemes, since the
915 knowledge accumulation ability is hampered by giving more emphasis to older tasks. However,
916 note that such a sub-optimal reverse weighting strategy is still better than the pure offline merging
917 strategy with *no replay*. This helps further ablate the exact importance of *replay* and *non-uniform*
weighting for improving pure offline-merging techniques in the presence of the time axis.

918
919
920
921
922
923
924
925
926
927
928



929
930
931
932
933
934
935
936
937
938
939
940
941
942
943
944
945
946
947
948
949
950
951
952
953
954
955
956
957
958
959
960
961
962
963
964
965
966
967
968
969
970
971

Figure 8: **Effect of reverse-weighting for offline merging techniques.** We find that reversing the weighting scheme that yielded consistent boosts from Fig. 7 is sub-optimal—indeed, it performs worse than the offline merging with replay methods.

E ADDITIONAL EMA EXPERIMENTS

E.1 TASKS AS DATASETS

In the main text, we presented all results using a data stream that randomly mixes concepts from different datasets into a coherent set of tasks—following the *random* data-stream in Roth et al. (2024b). Here, we relax this constraint and re-run our experiments using individual datasets as tasks, consistent with the standard model merging literature (Ilharco et al., 2022; 2023; Yadav et al., 2023). Specifically, we use the *dataset-incremental* stream from Roth et al. (2024b). Even in this setup, we reproduce our main findings. In Fig. 9, we confirm the results from Fig. 6, showing that all offline merging techniques perform poorly when exposed to the axis of time, failing to even match the performance of a simple continual fine-tuning *replay* baseline. Additionally, in Fig. 10, we corroborate the results from Fig. 3, demonstrating that the *best-in-TIME* method remains the most effective temporal model merging approach. We also confirm that the choice of model merging technique is far less critical for temporal model merging than the initialization and deployment strategies.

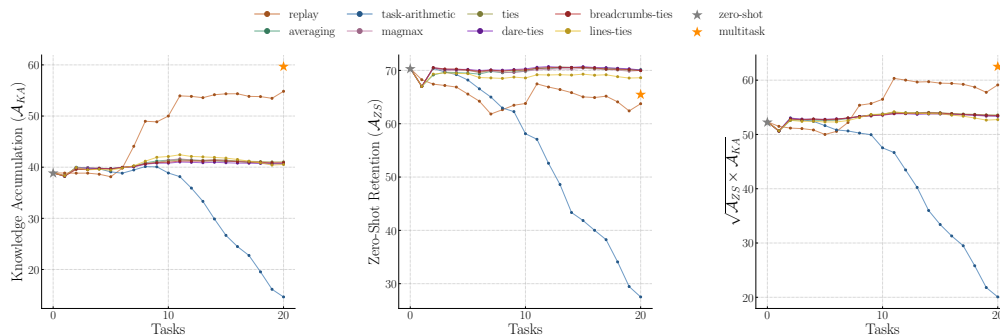
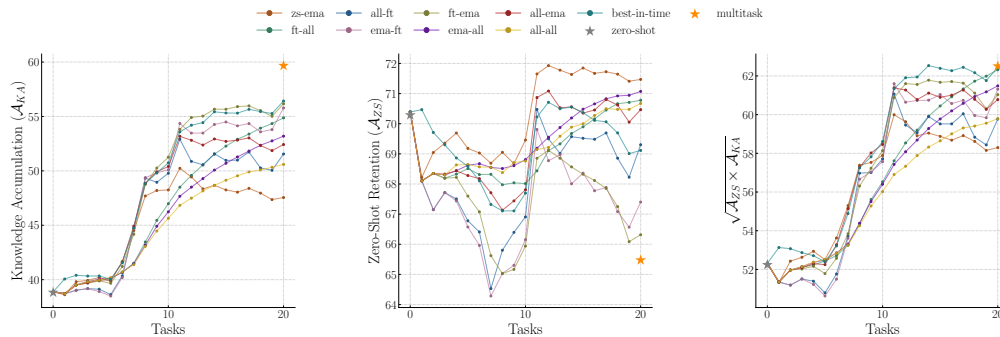


Figure 9: **Offline merging techniques still struggle in the tasks-as-datasets setting.** Switching from the *random* data-stream (Fig. 6 in the main paper) to the *dataset-incremental* stream, which aligns more closely with the standard multi-task merging literature setups, reveals that offline merging techniques still severely underperform compared to the simple *replay* baseline.

E.2 LONGER TASK SEQUENCES

To test the robustness of our findings in Sec. 3.2, we repeat the experiment shown in Fig. 3 on a longer sequence with the number of tasks $T = 50$ (Fig. 11). For 50 tasks, *Best-in-TIME* still strikes the optimal balance between knowledge accumulation and zero-shot retention. One notable difference with respect to Fig. 3 is the large initial advantage of the zero-shot initialization strategy combined with the EMA deployment strategy. When the learning horizon is further extended to 100

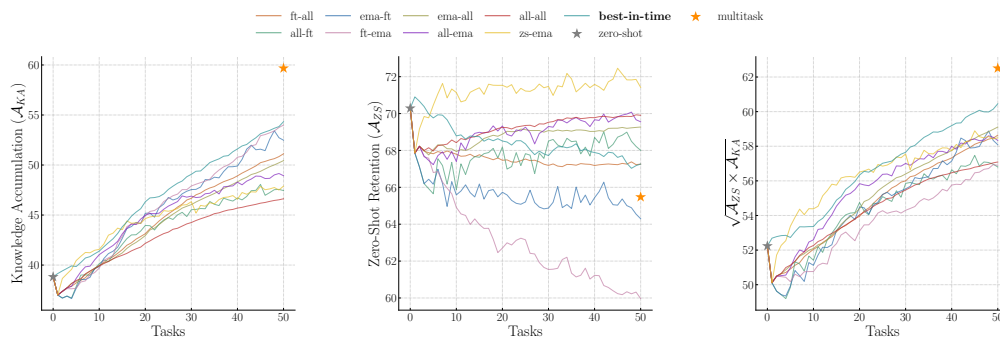
972
973
974
975
976
977
978
979
980
981
982



983
984
985
986
987
988
989
990

Figure 10: **Dataset-Incremental TIME Exploration.** We replicate the results from Fig. 3 using the dataset-incremental stream instead of the random stream. The main takeaways remain unchanged: initialization and deployment strategies primarily determine temporal merging performance, and the EMA-averaging initialization and deployment strategy utilized in *Best-in-TIME* is the best approach.

991
992
993
994
995
996
997
998
999
1000



1001
1002
1003
1004

Figure 11: **A long journey through TIME.** We compare all valid combinations of initialization and deployment protocols on a longer sequence of 50 tasks. *Best-in-TIME* remains the best in balancing knowledge accumulation and zero-shot retention.

1005
1006
1007
1008
1009
1010
1011

tasks, this initial advantage is maintained, establishing the zero-shot initialization approach as the best-performing method, as shown in Fig. 12. Although the double EMA variant surpasses zero-shot initialization in knowledge accumulation, its poor retention relegates it to third place on the combined metric. In this exploration we re-use the optimal interpolation weight from the 20 task scenario, which may no longer be ideal for longer horizons, as it directly influences the balance between knowledge accumulation and zero-shot retention.

1012

1013 E.3 VARIANCE ANALYSIS ACROSS RUNS

1014
1015
1016
1017
1018
1019
1020

To put our results from Sec. 3.3 in perspective, we quantify the variance across runs for a single merging method. Specifically, we run *Best-in-TIME* three times and show the mean and standard deviation across runs in Fig. 13. Comparing this to Fig. 4 reveals that the best results for different methods fall within the standard deviation of multiple runs of the same method. In particular, for the last task, the standard deviation of the geometric mean of knowledge accumulation and zero-shot retention is 0.96.

1021

1022 F HYPERPARAMETER DETAILS

1023
1024
1025

In an effort to remove any confounding factors, we conduct an extensive hyperparameter sweep, to the best of our abilities, for each individual merging technique for Figs. 4, 6 and 7. We list the hyperparameter ranges swept over for each technique below:

1026
 1027
 1028
 1029
 1030
 1031
 1032
 1033
 1034
 1035
 1036
 1037
 1038
 1039
 1040
 1041
 1042
 1043
 1044
 1045
 1046
 1047
 1048
 1049
 1050
 1051
 1052
 1053
 1054
 1055
 1056
 1057
 1058
 1059
 1060
 1061
 1062
 1063
 1064
 1065
 1066
 1067
 1068
 1069
 1070
 1071
 1072
 1073
 1074
 1075
 1076
 1077
 1078
 1079

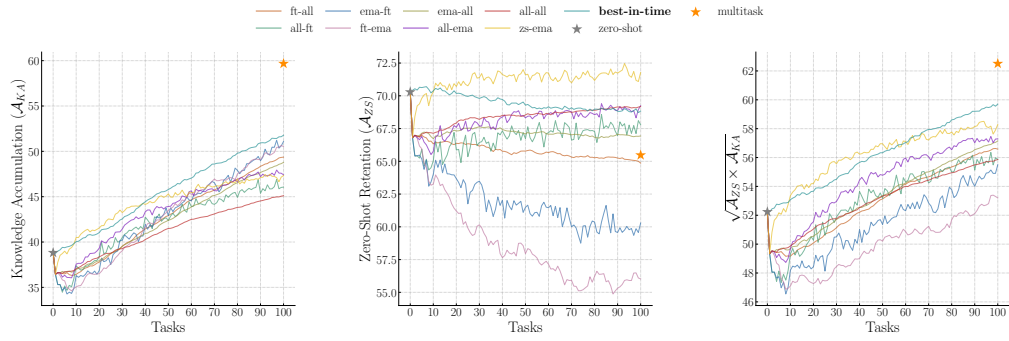


Figure 12: **An even longer journey through TIME.** We compare all valid combinations of initialization and deployment protocols on a longer sequence of 100 tasks. *Best-in-TIME* still remains the best approach balancing knowledge accumulation and retention, measured as the geometric mean of the two metrics in the right-most figure.

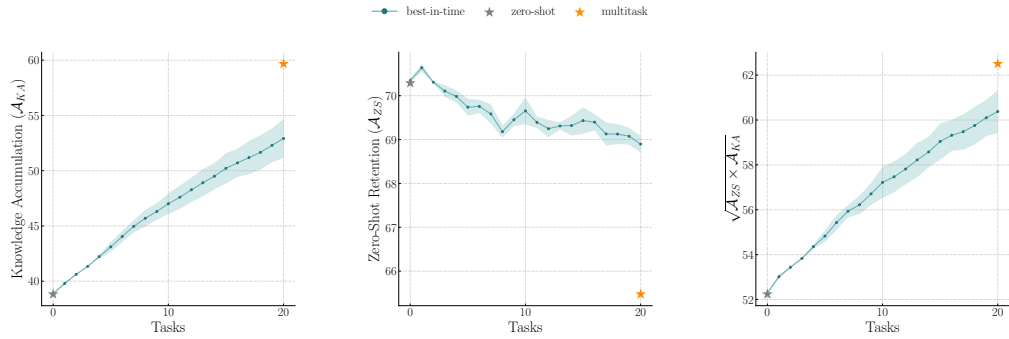


Figure 13: The mean and standard deviation across three runs of *Best-in-TIME*.

- **Weight Averaging.** For the offline merging, we use a standard merging coefficient of $\frac{1}{N}$, where N is the number of task checkpoints to merge.
- **SLERP.** In SLERP, as we can only merge two checkpoints at a time, we sweep over the following weight-coefficients: $\{0.1, 0.3, 0.5, 0.7, 0.9\}$.
- **Task-Arithmetic.** We sweep over the scaling factor: $\{0.1, 0.2, 0.3, 0.4, 0.5, 0.6, 0.7, 0.8, 0.9, 1.0\}$
- **TIES.** We sweep over the scaling factor: $\{0.1, 0.2, 0.3, 0.4, 0.5, 0.6, 0.7, 0.8, 0.9, 1.0\}$ and the pruning-fraction: $\{0.1, 0.2, 0.3, 0.4, 0.5, 0.6, 0.7, 0.8, 0.9, 1.0\}$.
- **DARE-TIES.** We sweep over the scaling factor: $\{0.1, 0.2, 0.3, 0.4, 0.5, 0.6, 0.7, 0.8, 0.9, 1.0\}$ and the pruning-fraction: $\{0.1, 0.2, 0.3, 0.4, 0.5, 0.6, 0.7, 0.8, 0.9, 1.0\}$.
- **Breadcrumbs-TIES.** We sweep over the scaling factor: $\{0.1, 0.2, 0.3, 0.4, 0.5, 0.6, 0.7, 0.8, 0.9, 1.0\}$ and the pruning-fraction: $\{0.1, 0.2, 0.3, 0.4, 0.5, 0.6, 0.7, 0.8, 0.9, 1.0\}$.
- **MagMax.** We sweep over the scaling factor: $\{0.2, 0.4, 0.8, 1.0\}$.
- **LiNeS-TIES.** We keep α fixed to 0.5, and sweep β : $\{0.2, 0.5, 0.8\}$ and prune-fraction: $\{0.2, 0.5, 0.8\}$ as recommended in the original paper (Wang et al., 2024a).